Polar Science 10 (2016) 262–269

Contents lists available at ScienceDirect

Polar Science

journal homepage: https://www.evise.com/profile/#/JRNL_POLAR/login

The accuracy of satellite-derived albedo for northern alpine and glaciated land covers

Scott N. Williamson [a, *], Luke Copland [b], David S. Hik [a]

[a] Department of Biological Sciences, University of Alberta, Edmonton, Alberta, T6G 2E9, Canada
[b] Department of Geography, Environment and Geomatics, University of Ottawa, Ottawa, Ontario, K1N 6N5, Canada

ARTICLE INFO

Article history:
Received 30 November 2015
Received in revised form
7 June 2016
Accepted 13 June 2016
Available online 15 June 2016

Keywords:
Albedo variability
Tundra
Glacier
MODIS

ABSTRACT

Alpine and Arctic land cover can present a challenge for the validation of satellite-derived albedo measurements due, in part, to the complex terrain and logistical difficulty of accessing these regions. We compared measurements of albedo on transects from northern mountain land covers (snowfield, glacier ice, tundra, saline silt river delta) and over a large elevation range to the coincident 8-day MODIS (MCD43) albedo product. We also compared field measurements at snow covered sites to the coincident daily MODIS (MOD10A1) snow albedo product. For each transect, we measured a range of albedo values, with the least variability on the silt river delta (range = 0.084) and the largest over mid-elevation glacier ice (range = 0.307). The highest elevation snowfield (0.170) had nearly the same range of albedo values as tundra (0.164). The MODIS shortwave White Sky Albedo product (MCD43A3) was highly correlated with the field transect albedo (R^2 = 0.96), with a Root Mean Square Error (RMSE) of 0.061. The MODIS shortwave Black Sky Albedo product was similarly correlated with field transects (R^2 = 0.96; RMSE = 0.063). These results indicate that remote observation of albedo over snow covered and alpine terrain is well constrained and consistent with other studies. Albedo varied by ~15% both spatially and temporally for the high elevation snowfields at the point in the season where albedo variation should be at its minimum. There were several instances where MCD43A3 albedo was not produced over snow and was instead classified as cloud covered, despite field observations of cloud free skies. There were also several instances where daily MOD10A1 albedo was produced during the coincident 8-day period at these locations. This suggests that the cloud mask in the MCD43 product is overly conservative over snow. Spatial variation in albedo within the MODIS grid cell (500 m), especially for snow and glacier ice, combined with the uncertainty associated with positional accuracy of MODIS, indicates that the accuracy of MODIS albedo will be dependent on both land cover type and the period of observation.

1. Introduction

Determining the Earth's albedo is most efficiently undertaken by satellite remote sensing, but assessing the accuracy of such measurements is challenging, particularly in complex terrain. Climate modeling relies on the accurate determination of albedo. The values typically used for characterizing the accuracy of land surface albedo in general circulation models are in the range of ±0.05 (Henderson-Sellers and Wilson, 1983) to ±0.02 (Sellers, 1993). Barry (1985) recommends an albedo accuracy of 0.02 for snow cover modeling. Constraining the accuracy of albedo measurements is therefore important, and there are several methods for validating coarse spatial resolution satellite albedo products. Satellite data can be compared to field measurements of albedo, or compared to finer spatial resolution albedo which is often collected at a more coarse temporal resolution from satellite or aircraft.

Field measurements of albedo are commonly calculated from upward and downward facing broadband pyranometers sensitive to the visible and near-infrared portion of the electromagnetic spectrum. The advantage of this technique is that conditions influencing surface albedo (e.g., solar zenith angle, surface properties and atmospheric conditions) can be identified and constrained. These field measurements are typically made at either a stationary meteorological station or with a mobile sampling apparatus. One of the few examples of spatial and temporal

* Corresponding author.
E-mail address: snw@ualberta.ca (S.N. Williamson).

http://dx.doi.org/10.1016/j.polar.2016.06.006
1873-9652/

sampling of albedo variability across the accumulation and ablation zones of a glacier is from Haut Glacier d'Arolla, Switzerland, where Brock et al. (2000) reported that albedo can vary by as much as 20–30% across a 500 m transect for some sections of the glacier at particular times of year. Spatial sampling of albedo across snow covered Alaskan tundra (Sturm et al., 2005) using pyranometers suspended on 50 m cable transects indicated variability in albedo of nearly 90% across tundra with residual spring snow patches.

Several studies have compared spatial albedo ground sampling to satellite derived albedo. For example, Lucht et al. (2000) sampled grasslands and shrublands with various degrees of visible soil and compared the results to AVHRR derived albedo. They found that the field albedo data varied by up to 0.08 and that the field measurements agreed with AVHRR values within ±0.05. Liang et al. (2002) compared field measurements of albedo and LandSat ETM + albedo to validate MODIS albedo measurements for the USDA Agricultural Research Centre in Beltsville, MD, USA, with the land cover types including soils, crops, natural vegetation and urban. They reported an accuracy between MODIS albedo and the validation measurements of <0.05, in most instances.

Validation of MODIS-derived snow and ice albedo values on the Greenland Ice Sheet using pyranometer-derived albedo from stationary meteorological stations (Stroeve et al., 2005, 2006, 2013) have been conducted assuming that the albedo of high elevation ice sheets is more homogeneous than other land cover types. The pyranometer used in these studies was the LI-COR 200SZ which has a spectral range of 0.4–1.1 μm, and which requires a correction to convert to the full short wave spectrum. Although the corrections are well understood and likely introduce little error, the field measurements do not share the same spectral range as MODIS total short wave albedo, which is 0.3–5.0 μm spread across 7 spectral bands. Stroeve et al. (2013) report an RMSE of 0.067 for high quality MCD43 data (combined MODIS Terra and Aqua at 500 m resolution) in comparison with *in situ* albedo data. Stroeve et al. (2005) reported a RMSE of 0.04 for *in situ* data versus MODIS Terra (MOD43) generated data. Post-processing of MODIS geolocation in conjunction with ground control points produces a positional error of approximately 50 m (1σ) at nadir for Terra and approximately 65 m for Aqua (Wolfe et al., 2002), although the positional error of low-resolution albedo products is likely not larger than 125 m (Stroeve et al., 2006).

High latitude alpine areas are typically difficult to access and are poorly covered by meteorological monitoring stations, which make continuous measurements of albedo rare. Furthermore, issues related to spatial scale are difficult to assess because it is logistically challenging to access these remote areas to conduct albedo sampling. Here we report on albedo measurements made in transects over a range of alpine and glaciated terrain in the southwest Yukon, Canada. These observations are compared with concomitant MODIS albedo values. Our primary objective was to determine the spatial variability in albedo within a MODIS grid cell of different alpine land covers. Our secondary objective was to compare and validate MODIS derived albedo values over a wide range of elevations and alpine land covers.

2. Methods

2.1. Field measurements and study area

Albedo was measured along transects at six locations in alpine and glaciated terrain in the southwest Yukon in summer 2013 and 2015 under a variety of cloud cover conditions (Table 1; Fig. 1; Fig. 2). The measurement locations were purposely chosen in regions that had low slopes (<5°), consistent aspects and were >1 km from large changes in elevation or land cover. These locations are therefore considered to be representative of the surface type being measured and were far enough away from other land surfaces to avoid contamination from adjacent land cover types within 500 × 500 m MODIS grid cells. The transects consisted of parallel or perpendicular lines, with albedo measurements made approximately every 30–50 m. The transects ranged between 200 m and 1000 m in length, and each location had at least one transect that was 500 m in length. The sampling regime could not be precisely replicated at each sample location due to hazards from features such as meltwater channels and crevasses.

Albedo measurements were made with a CMA11 instrument (Kipp & Zonen, Delft, The Netherlands) mounted on a portable tripod, with the differential voltage output connected to a CR10X data logger (Campbell Scientific, Logan, Utah). The albedo measurement apparatus is shown in the foreground in Fig. 2 (panels C & E). The CMA11 consists of an upward and a downward facing secondary class pyranometer that is sensitive to wavelengths in the 0.300–2.400 μm range of solar radiation. This pyranometer is the highest precision class solar radiation measurement instrument manufactured by Kipp & Zonen. The logger was programmed to record incoming and reflected solar radiation every minute, as the average of five second samples. The logger clock was synchronized with a wrist watch, and moved at approximately 10 min intervals along each sampling transect. The location of each site was recorded with a handheld GPS.

To determine representative minimum surface albedo values, measurements should ideally be taken under direct sunlight and cloud free conditions, and close to diurnal minimum zenith angle. The land covers in this study fall into two broad types: snow and ice, and partially vegetated barren ground. Increasing the solar zenith angle acts to increase albedo on these land cover types (e.g., Ohmura, 1981; Dozier, 1989; Carroll and Fitch, 1981). Consequently, albedo measurements were made within ~3 h of local solar noon to minimize sun illumination effects caused by comparing measurements made at variable zenith angles, or from zenith angles greater than ~50° (Brock et al., 2000). Solar zenith angles greater than 70° have been shown to cause degradation in the quality of MODIS albedo (Stroeve et al., 2005, 2006). Similarly, Wang and Zender (2010) suggest that while the spatiotemporal patterns of MODIS albedo may be correct for large solar zenith angles, the accuracy may deteriorate for angles > 55° and may become physically unrealistic for angles > 65°. In our study, the values for solar zenith angle are almost entirely <55° (Table 1), likely mitigating much of this uncertainty. However, we are aware that the relationship between solar zenith angle and surface albedo observations is complex (e.g., Cronin, 2014).

Changing atmospheric and surface conditions also influence albedo. Cloud cover affects snow and dry tundra vegetation albedo differently. For an increase in solar elevation angle at small angles (from 10° to 40°) under complete cloud cover, snow albedo increases by up to ~2% (Choudhury and Chang, 1981); in general snow albedo for cloudy skies is a few percent higher than those from under clear skies. Under diffuse solar radiation caused by cloud cover vegetation albedo can be decreased by up to ~2% (Eugster et al., 2000). The albedo of bare soil increases as it dries, a phenomenon which is observed both diurnally and seasonally (Eugster et al., 2000). The albedo of snow is primarily determined by grain size, where weathering of fresh snow increases grain size and decreases albedo (e.g., Dozier, 1989).

Details of the sample locations are listed in Table 1 and shown in Fig. 2. The high elevation snowfield location A (accumulation zone of the Kaskawulsh Glacier) was measured on August 8, 2015. This site consisted of flat, wet, partially weathered snow. The ablation region of the Kaskawulsh Glacier was measured at an elevation of 1370 m on August 9, 2015 (Site E). This site comprised glacier ice

Table 1
Characteristics of each measurement site. The letters in parenthesis indicate the location in the study area (Fig. 1). The number of distinct albedo measurement locations at each site are indicated, as well as the hemispherical cloud cover over the measurement interval of several hours around local solar noon.

Site (letters on Fig. 1)	Date	Day of year	Start time Stop time	Latitude Longitude	Average elevation (m a.s.l.)	Number of observations	Cloud cover	Solar zenith range (°)
Snowfield (A)	August 8, 2015	220	11:25 14:40	60.69N139.79W	2597	12	Clear	44.59–54.16
Snowfield (B)	August 16, 2015	228	12:28 12:44	60.48N138.92W	2485	2	Mixed	47.16–47.70
Tundra (C)	July 14 & 15, 2013	195 & 196	13:55–16:48 12:26–16:23	61.21N138.28W	1620	25	Clear	40.12–60.50
Lowell Glacier (D)	August 16, 2015	228	9:38 11:52	60.33N138.61W	1515	9	Mixed	52.28–46.46
Kaskawulsh Glacier (E)	August 9, 2015	221	12:39 14:41	60.72N138.82W	1370	11	Overcast	45.60–54.16
Saline Silt Delta (F)	August 13, 2015	225	12:36 14:45	61.00N138.50W	780	12	Clear	46.92–55.74

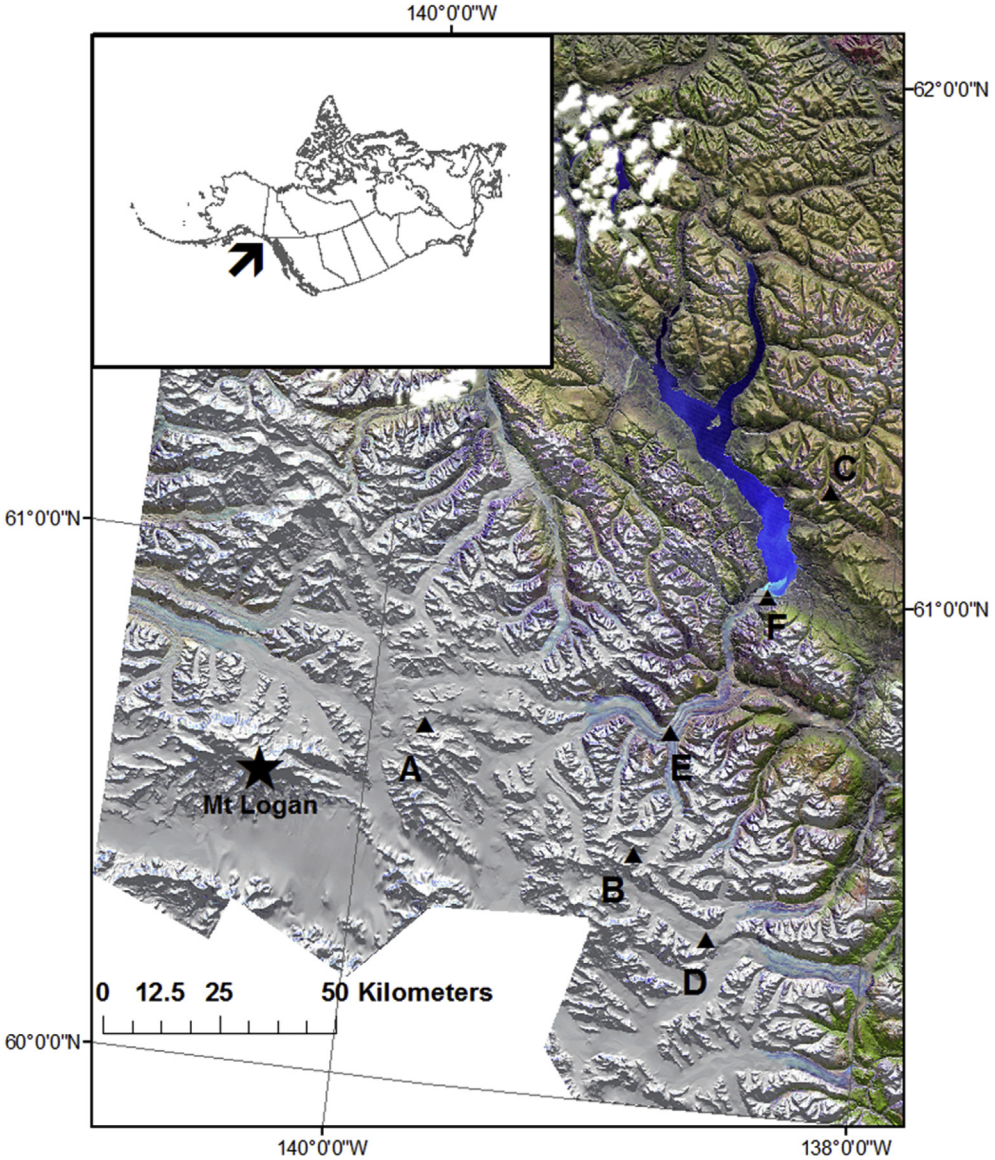

Fig. 1. Study area in the southwest Yukon (arrow in inset map of Canada) showing sampling sites A–F, which are described in Table 1. Mount Logan, Canada's highest mountain (5959 m) is marked by the star.

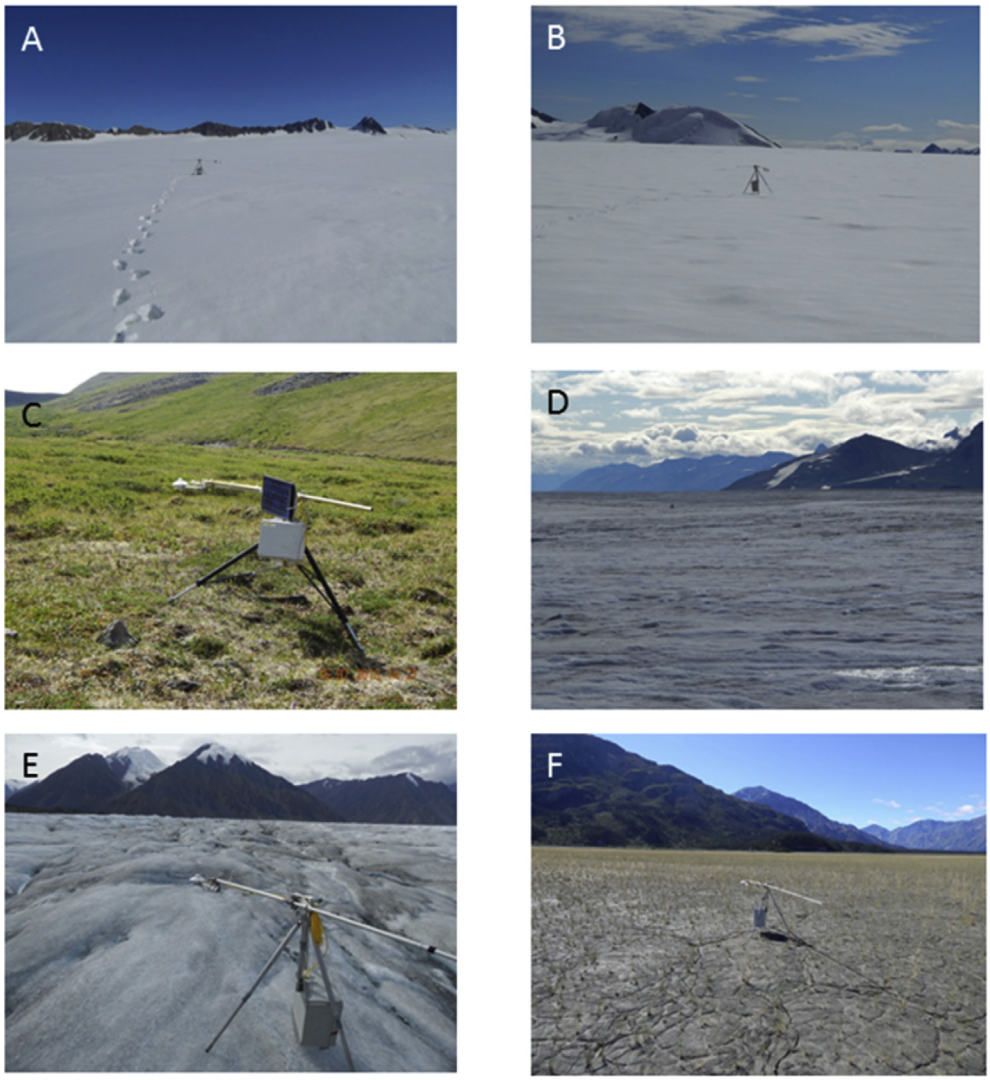

Fig. 2. Photographs of the landscape cover for sites A-F. The albedo measurement apparatus is clearly visible in pictures C and E.

with weathered snow on high features and mud in the bottom of water filled supraglacial channels, and small meltwater ponds. The Slims River delta (Site F) at the south end of Kluane Lake was comprised of sparsely vegetated saline silty loam (Harris, 1990), and was measured on August 13, 2015. A mid-glacier location on Lowell Glacier (Site D) was measured on August 16, 2015; this location was near the glacier's equilibrium line and composed of dense, metamorphosed snow, with many small crevasses and surface depressions. No melt channels or melt debris was evident. Measurements at Site B, in the upper accumulation zone of the South Arm of the Kaskawulsh Glacier, were made on August 16; due to limited helicopter availability at this location only two point albedo measurements were completed. The appearance of this location was very similar to snowfield location A. The alpine tundra transect C was measured on July 14 and 15, 2013. This location was dominated by dry tundra, sedge, short statured shrubs, and barren ground (Williamson et al., 2016). Very little standing water was present near this transect and lichen-covered talus comprised approximately 20% of the ground surface. In the absence of new snowfall at any of the icefield or glacier locations and minimal rainfall at the tundra (<1.8 mm) and delta locations (<11.5 mm; measured 5 km away at Kluane Lake Research Station) during the 8-day MODIS aggregation periods, we assume that surface albedo showed little change within these periods. Solar zenith angles are provided in Table 1, calculated using the on-line version of the National Oceanic and Atmospheric Administration's Solar Calculator (http://www.esrl.noaa.gov/gmd/grad/solcalc/azel.html).

2.2. MODIS albedo data

Both MODIS MCD43 and MOD10 albedo were used in this study. The first type is the version 5, 500 m grid, 8-day composite MCD43A3, which uses both MODIS Aqua and Terra imagery as input. The 8-day product is produced from the Bidirectional Reflectance Distribution Function (BRDF) and MCD43A1 albedo model parameter product (Schaaf et al., 2011; Schaaf et al., 2002). If the MODIS daily cloud masks determine that a grid cell is cloud free, then an albedo value is produced. The MODIS BRDF values are converted to White-sky and Black-sky albedos. White-sky albedo is the bihemispherical reflectance under isotropic illumination conditions and therefore has the angular dependency eliminated. The black-sky albedo is the directional hemispherical reflectance which for the MODIS MCD43A3 product is calculated for local solar noon. In more general terms, black sky albedo is produced as a function of

solar zenith angle in the absence of diffuse solar radiation, while white sky albedo refers to conditions when diffuse solar radiation is isotropic and there is an absence of direct beam solar radiation. The albedo produced is either the full inversion BRDF (high quality flag) or the magnitude inversion (poor quality flag), which is employed when insufficient observations are available to produce the full inversion. The magnitude inversion is produced with an *a priori* knowledge backup algorithm and performs well under most circumstances (Jin et al., 2003a,b). The MODIS MCD43A2 quality flag was used to determine the BRDF quality for all of the MODIS albedo values used in this study.

The second type of MODIS albedo used here is the daily MOD10A1 snow albedo produced from the MODIS sensor on the Terra platform (Hall et al., 2002). The daily MOD10A1 snow albedo is produced only for locations with permanent snow and ice which corresponds to sites A, B, D and E, and for areas determined by the MODIS cloud mask (MOD35) to be cloud free. The MOD10A1 snow albedo is produced from the highest scoring single daily observation, based on an algorithm based on viewing and illumination angles in addition to cloud information.

3. Results

Albedo was measured on four land cover types (saline silt delta, glacier ice, tundra, snowfield), spanning an elevation range of 780 m to 2597 m. The field (*in situ*) albedo data are summarized in Table 2 and MODIS albedo data is summarized in Tables 3 and 4. Interestingly, the highest elevation snowfield had a similar range of albedo values as tundra (0.170 and 0.164, respectively). Albedo was least variable for the silted delta (range = 0.084) and most variable over mid-elevation glacier ice (range = 0.307). The albedo range of snowfield location B should be interpreted more cautiously because only two measurements were made at that location, but is still included here for comparison. The distribution of the average albedo values from each location within each site (Fig. 3) shows that the variability in albedo is site dependent.

The MODIS shortwave White Sky Albedo product (MCD43A3) was highly correlated with the field transect albedo ($R^2 = 0.96$) with a Root Mean Square Error (RMSE) of 0.061 (Fig. 4a). The MODIS shortwave Black Sky Albedo product was similarly correlated with field transects ($R^2 = 0.96$; RMSE = 0.063; Fig. 4b). Investigation of the MODIS albedo quality flag product (MCD43A2) for the grid cells used in the study indicates that only one grid cell for the Kaskawulsh Glacier (Site D) had the full BRDF inversion. This grid cell contained 9 of the 11 *in situ* measurements from this location. The remaining MODIS grid cells used in this study were the poor quality magnitude inversion albedo values.

The two highest elevation snowfield locations (sites A and B) did not have intersecting MCD43A3 albedo values produced using either inversion method. Using a digital elevation model and LandSat TM imagery, four adjacent MODIS albedo grid cells were therefore chosen based on the similarity of elevation and slope to the field sampling location. These four MODIS albedo grid cells were compared to the field albedo values, and were located approximately 2.5 km from field site A and 6.0 km from field site B. The proxy grid cells at Site A were less than 100 m lower in elevation than the measurement site. The proxy grid cells at Site B were approximately 400 m lower in elevation.

Albedo for the snow covered sites was also investigated using the daily snow albedo product produced from MOD10A1 (Table 4; Fig. 4). MOD10A1 albedo values were present for three of the four sites for the same day that field albedo was measured. This includes Snowfield location A, where MCD43A3 albedo was not produced over the coincident 8-day aggregation period. Although snowfield location B didn't have MOD10A1 albedo produced on the same day as field measurements, the daily snow albedo was produced for four days of the 8-day MCD43 aggregation period, even though MCD43A3 albedo was not produced for this location. The range between maximum and minimum MOD10A1 albedo over the 8-day MCD43 aggregation period was as large for the apparently homogeneous snowfields as it was for the Kaskawulsh Glacier (site E) which exhibited standing water, melt channels and accumulations of gravel and mud. The MOD10A1 albedo values are superimposed over the MCD43A3 albedo values on Fig. 4. Substituting MOD10A1 albedo values for MDC43A3 for the snow covered sites changed the RMSE to 0.074 (retaining White Sky Albedo for sites C & F) and 0.075 (retaining Black Sky Albedo for sites C & F).

4. Discussion

Our comparisons between field and remotely derived albedo have similar RMSE (±0.06) to other studies which use orders of magnitude more data (Stroeve et al., 2005, 2013; Liang et al., 2005). This suggests that a fundamental limit in albedo validation exists for surfaces that exhibit a large variation in spatial albedo, with an RMSE of 0.06 likely nearing the highest accuracy that can be achieved using MODIS albedo of all quality states, although an accuracy of ±0.04 (RMSE) has been reported by Stroeve et al. (2005) for high quality full BRDF inversion on the Greenland Ice Sheet. The large uncertainty in MODIS positional accuracy of between 50 m and 125 m, coupled with land covers that display a large range of albedo values within a MODIS 500 m grid cell and over an 8-day aggregation period, indicates that a MODIS albedo accuracy of ±0.02 is unlikely to be achieved for modeling of snow cover, tundra or glacier surfaces, and for GCM input (Sellers, 1993; Barry, 1985). Relatively homogeneous land covers such as the silted delta could produce an albedo accuracy nearing ±0.02, whereas the more variable glacier surfaces will likely have an accuracy limit larger than that of tundra. The spatial and temporal variability in albedo for snowfields is much larger than their homogeneous appearance initially suggests, meaning that they have an albedo accuracy similar to glaciers and tundra.

The field albedo measurements are not likely affected by large zenith angles, because measurements were made within several hours of solar noon, when angles were close to 50° and much less than 70°. For the zenith angle ranges under which measurements

Table 2
Albedo statistics for the measurements made at the field sites listed in Table 1 and Fig. 1. Site B (*) only had two albedo measurements, so the uncertainty in the albedo variability at this location is poorly constrained.

Site (letters on Fig. 1)	Average albedo	Standard deviation	Minimum	Maximum	Range
Snowfield (A)	0.742	0.052	0.661	0.831	0.170
Snowfield (B)*	0.671	0.021	0.656	0.686	0.030
Tundra (C)	0.168	0.038	0.062	0.226	0.164
Lowell Glacier (D)	0.426	0.072	0.324	0.580	0.256
Kaskawulsh Glacier (E)	0.281	0.100	0.105	0.412	0.307
Saline Silt Delta (F)	0.106	0.027	0.076	0.160	0.084

Table 3
MODIS albedo (MCD43) statistics for the 8-day composite MODIS 500 m grid cells which intersect the field measurements locations for White Sky Albedo (WSA) and Black Sky Albedo (BSA). The 4* indicates the number of adjacent grid cells of similar geographical properties that were sampled for the two snowfield sites when no intersecting MODIS albedo values were available.

Site (letters on Fig. 1)	MCD43 8-day (start date)	MCD43 grid cells	MODIS BDRF quality Flag	WSA average	WSA st dev	BSA average	BSA st dev
Snowfield (A)	217	4*	Magnitude	0.815	0.014	0.804	0.013
Snowfield (B)	225	4*	Magnitude	0.639	0.019	0.631	0.019
Tundra (C)	193	2	Magnitude	0.145	0.001	0.137	0.001
Lowell Glacier (D)	225	3	Magnitude	0.318	0.008	0.312	0.010
Kaskawulsh Glacier (E)	217	2	Full (One grid cell) Magnitude (One grid cell)	0.215	<0.001	0.213	0.001
Saline Silt Delta (F)	225	5	Magnitude	0.104	0.005	0.104	0.005

Table 4
MODIS (MOD10A1) daily snow albedo for the snow and ice covered sites. Average snow albedo for the days of field albedo measurement and 8-day averages coincident with the MCD43 aggregation period are included.

Site (letters on Fig. 1)	MCD43 8-day period	MOD10A1 count in MCD43 8-day period	MOD10A1 grid cells	MOD10A1 albedo average from field sample day	MOD10A1 albedo st dev from field sample day	MOD10A1 albedo 8-day average	MOD10A1 albedo 8-day st dev	MOD10A1 albedo 8-day Max	MOD10A1 albedo 8-day Min
Snowfield (A)	217–224	3	3	0.79	0	0.73	0.08	0.79	0.63
Snowfield (B)	225–232	4	1	Cloud covered	Cloud covered	0.67	0.04	0.71	0.61
Lowell Glacier (D)	225–232	6	2	0.30	0	0.26	0.04	0.33	0.16
Kaskawulsh Glacier (E)	217–224	3	3	0.17	0.03	0.21	0.03	0.25	0.12

were made (40°–60°; Table 1) we expect that the variation in albedo would be no greater than 10% (Warren, 1982; Aoki et al., 1999). This effect would be greatest for snow/ice surfaces that have melted and for those which have large grain sizes. These types of surfaces were measured under a solar zenith angle range of approximately 45°–55°, which indicates that the variation in albedo would be less than 10% for the 40°–60° range. The MCD43 product does not include information concerning zenith angle or time of capture, which makes it impossible to evaluate the dependency of MODIS albedo zenith angle in this study. Overcast conditions may have increased the albedo of the snow and ice at sites D & E. For example, Fig. 4 shows that sites D and E are to the right of the 1:1 line, which is consistent with an albedo increase from overcast and cloudy sky conditions. If these sites had been sampled under direct sunlight and clear skies, sites D and E could have appeared up to 2% closer to the 1:1 line. However, this would not have significantly improved the RMSE.

The validation period used here coincides with the time of year when surface albedo has stabilized. The vegetation canopy will have reached maturity and soil moisture values will be nearing minimum, both seasonally and diurnally. The periodic snowfall events common to alpine regions are also at a minimum. Thus the albedo measurements made on a single day will be more similar to the MODIS 8-day composite than if the comparisons were made in the spring or later in the summer.

Although we found a strong correlation between field albedo measurements and MODIS White-sky and Black-sky albedo, a small improvement between MODIS and field albedo measurements might be feasible if Blue-sky albedo was calculated from MODIS White-sky, Black-sky and aerosol optical depth (Román et al., 2010). Furthermore, if full inversion (high quality flag) MODIS data had been available for every field site, instead of only 1 of the 6 locations measured, a further improvement of the correlation would be expected.

The high correlation found between *in situ* and MODIS albedo originating from all quality classes indicates that the poorer quality magnitude inversion albedo values perform well for a range of alpine and glaciated land covers. This is despite the fact that we had to use surrogate MODIS albedo grid cells for the two snowfield locations (sites A and B), which likely influenced the relationship between MODIS and *in situ* values due to small differences in factors such as snow weathering, elevation and aspect. Similarly, some variability will occur between MODIS and field measurements because the direct average of field measurements has not been weighted by the cover percentages within the grid cell.

The case of missing albedo values for snowfields where clear skies were confirmed is suggestive of snow covered areas being confused with cloud cover, at least for the MCD43A3 product. The MODIS Albedo Theoretical Basis Document (https://lpdaac.usgs.gov/dataset_discovery/modis/modis_products_table/mcd43a3) indicates that the albedo product will aggregate all atmospherically corrected and cloud-cleared surface reflectance observations. Ground based observations within the grid cells that were not assigned MODIS albedo values were confirmed to be clear sky for at least one day within the 8-day aggregation period for both Terra and Aqua overflights. Furthermore MOD10A1 albedo was produced 3 and 4 times at Snowfield sites A and B, respectively, indicating that the cloud mask is likely being used too conservatively in the MCD43A3 product.

Future research should consider the potential for confusion of snow cover with cloud cover and cloud contamination of the albedo product. This task should be broken into two distinct lines of investigation: i) contamination of high quality MODIS albedo and ii) the incorrect cloud masking of valid surface albedo. The highest quality MODIS Land Surface Temperature data from our study area have been shown to be cloud contaminated (Williamson et al., 2013), suggesting that MODIS albedo also contains a small amount of residual cloud contamination. Furthermore, some valid

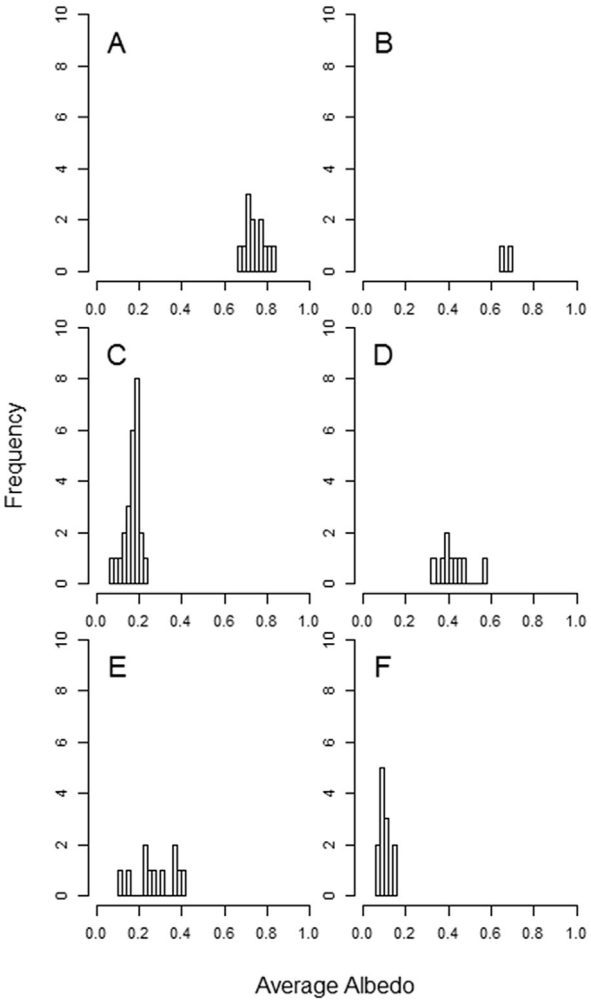

Fig. 3. Histogram of the average albedo, from field measurements, for each location within sites A-F. Summary statistics can be found in Tables 1 and 2

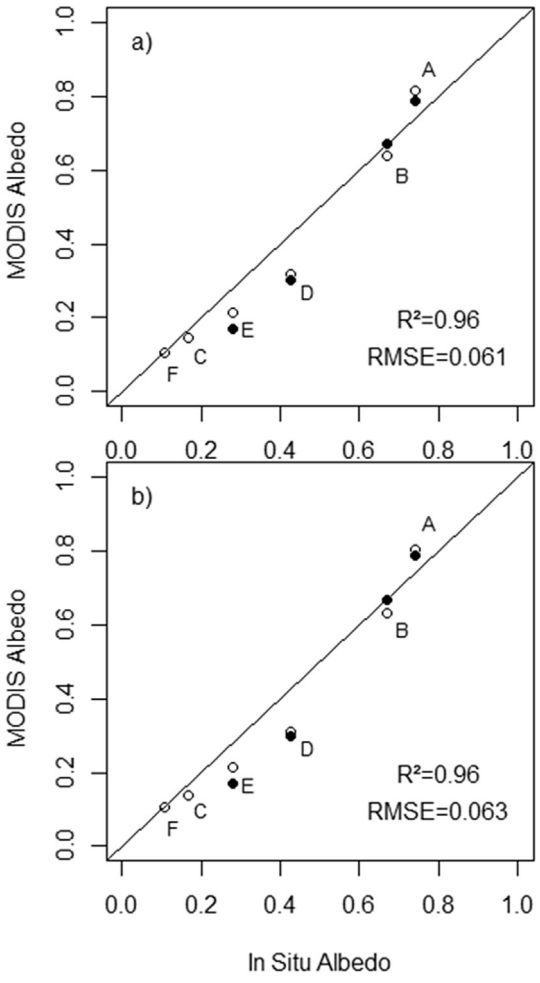

Fig. 4. The correlation and Root Means Square Error between spatially average 8-day MCD43A3 White Sky Albedo (a), Black Sky Albedo (b) and the average of field albedo measurements are shown as open circles. The closed black circles are the daily MOD10A1 snow albedo. Sites A, D, and E albedo values (MOD10A1 – black circles) from the same day as field measurements. Site B is the 8-day average of MOD10A1, because the day corresponding to field measurements was labeled as cloud cover. The black solid line in both plots represents the 1:1 line. Information regarding measurements at sites A–F can be found in Tables 1, 2, 3 and 4, and Fig. 3 shows the histogram of the in-situ albedo values by location within each site.

surface albedo data are likely confused with cloud cover and rejected. The extent of this problem is more difficult to resolve because cloud cover and unassigned surface values in the albedo product are assigned a single fill value. Lastly, the minimum satellite derived albedo accuracy should correlate positively to the within grid-cell albedo range, modified for the positional accuracy of the satellite. However, we did not have enough field data to test this hypothesis.

5. Conclusions

Field measurements of albedo show that different land covers display a large variability at the spatial scale of a 500 m MODIS grid cell. This phenomenon, taken in combination with the positional accuracy of the MODIS satellites (Terra and Aqua), suggests that a fundamental limit to the accuracy of MODIS albedo is likely near to ±0.05 for snowfields and tundra; however the accuracy will be dependent on the albedo spatial variability of the land cover under consideration. Homogeneous surfaces such as the silted delta examined here produced better accuracy than snowfields, which did not have as homogeneous an albedo field as anticipated. More variable surfaces such as debris covered glacier ice will produce poorer accuracy. We also found evidence for inaccurate cloud masking in the MCD43A3 product over snow which indicates that future work is necessary to assess if the cloud mask is being used too conservatively. Finally, the addition of a zenith angle layer in the MODIS albedo product would aid in its validation.

Acknowledgements

We thank the Polar Continental Shelf Project (PCSP), Natural Resources Canada, for funding helicopter transportation. Financial support was also provided through the NSERC Discovery Grant program. The W. Garfield Weston Foundation and Wildlife Conservation Society of Canada provided funds for the purchase of the CMA11. Ellorie McKnight helped in conducting field measurements. Rainfall measurements were provided by Dr. Gwenn Flowers. Dion Parker with TransNorth Helicopters showed exceptional skill in accessing difficult to reach sites which made albedo measurements at high elevation snowfields possible. We thank two anonymous reviewers for helpful comments.

References

Aoki, T.E., Aoki, T.A., Hukabori, M., Uchiyama, A., 1999. Numerical simulation of the atmospheric effects on snow albedo with a multiple scattering radiative transfer model for the atmosphere-snow system. J. Meteor. Soc. Jpn. 77, 595–614.

Barry, R.G., 1985. Detecting the Climate Effects of Increasing CO_2. DOE/ER-0235. Department of Energy, Washington, D.C, pp. 109–141.

Brock, B.W., Willis, I.C., Sharp, M.J., 2000. Measurements and parameterization of albedo variations at Haut Glacier d'Arolla. Switz. J. Glaciol. 46, 675–688.

Carroll, J.J., Fitch, B.W., 1981. Effects of solar elevation and cloudiness on snow albedo at the South Pole. J. Geophys. Res. 86, 5271–5276.

Choudhury, B.J., Chang, A.T.C., 1981. The albedo of snow for partially cloud skies. Boundary Layer Meteorol. 20, 371–389.

Cronin, T.W., 2014. On the choice of average solar zenith angle. J. Atmos. Sci. 71, 2994–3003.

Dozier, J., 1989. Remote sensing of snow in visible and near-infrared wave-lengths. In: Asrar, G. (Ed.), Theory and Applications of Optical Remote Sensing. John Wiley and Sons, New York, pp. 527–547.

Eugster, W., Rouse, W.R., Pielke, R.A., McFadden, J.P., Baldocchi, D.D., Kittel, T.G.F., Chapin, F.S., Liston, G.E., Vidale, P.L., Vaganov, E., Chambers, S., 2000. Land-atmosphere energy exchange in Arctic tundra and boreal forest: available data and feedbacks to climate. Glob. Change Biol. 6, 84–115.

Hall, D.K., Riggs, G.A., Salomonson, V.V., DiGirolamo, N.E., Bayr, K.A., 2002. MODIS snow-cover products. Remote Sens. Environ. 83, 181–194.

Harris, S.A., 1990. Dynamics and origin of saline soils on the Slims River delta, Kluane national park, Yukon Territory. Arctic 43, 159–173.

Henderson-Sellers, A., Wilson, M.F., 1983. Surface albedo for climate modeling. Rev. Geophys. 21, 1743–1778.

Jin, Y., Schaaf, C.B., Woodcock, C.E., Gao, F., Li, X., Strahler, A.H., et al., 2003a. Consistency of MODIS surface BRDF/Albedo retrievals: 1. Algorithm performance. J. Geophys. Res. 108, D54158. http://dx.doi.org/10.1029/2002JD002803.

Jin, Y., Schaaf, C.B., Woodcock, C.E., Gao, F., Li, X., Strahler, A.H., et al., 2003b. Consistency of MODIS surface BRDF/Albedo retrievals: 2. Validation. J. Geophys. Res. 108, D54159. http://dx.doi.org/10.1029/2002JD00280.

Liang, S., Fang, H., Chen, M., Shuey, C.J., Walthall, C., Daughtry, C., Morisette, J., Schaaf, C., Strahler, A., 2002. Validating MODIS land surface reflectance and albedo products: methods and preliminary results. Remote Sens. Environ. 83, 149–162.

Liang, S., Stroeve, J., Box, J.E., 2005. Mapping daily snow/ice shortwave broadband albedo from moderate resolution imaging spectroradiometer (MODIS): the improved direct retrieval algorithm and validation with Greenland in situ measurement. J. Geophys. Res. 110, D10109. http://dx.doi.org/10.1029/2004JD005493.

Lucht, W., Hyman, A.H., Strahler, A.H., Barnsley, M.J., Hobson, P., Muller, J.-P., 2000. A comparison of satellite-derived spectral albedos to ground-based broadband albedo measurements modeled to satellite spatial scale for a semidesert landscape. Remote Sens. Environ. 74, 85–98.

Ohmura, A., 1981. Climate and Energy Balance of Arctic Tundra. Zürcher Geographische Schriften/ETH Zürich, Switzerland.

Román, M.O., Schaaf, C.B., Lewis, P., Gao, F., Anderson, G.P., Privette, J.L., et al., 2010. Assessing the coupling between surface albedo derived from MODIS and the fraction of diffuse skylight over spatially-characterized landscapes. Remote Sens. Environ. 114, 738–760.

Schaaf, C.B., Gao, F., Stahler, A.H., Lucht, W., Li, X., Tsang, T., et al., 2002. First operational BRDF, albedo and Nadir reflectance products from MODIS. Remote Sens. Environ. 83, 135–148.

Schaaf, C.L.B., Liu, J., Gao, F., Strahler, A.H., 2011. MODIS albedo and reflectance anisotropy products from Aqua and Terra. In: Ramachandran, B., Justice, C., Abrams, M. (Eds.), Land Remote Sensing and Global Environmental Change: NASA's Earth Observing System and the Science of ASTER and MODIS. Remote Sensing and Digital Image Processing Series, 11. Springer-Verlag, p. 873.

Sellers, P.J., 1993. Remote Sensing of the Land Surface for Studies of Global Change. NASA/GSFC International Satellite Land Surface Climatology Project Report, Columbia, MD.

Stroeve, J., Box, J.E., Gao, F., Liang, S., Nolin, A., Schaaf, C., 2005. Accuracy assessment of the MODIS 16-day albedo product for snow: comparisons with Greenland in situ measurements. Remote Sens. Environ. 94, 46–60.

Stroeve, J., Box, J.E., Haran, T., 2006. Evaluation of the MODIS (MO10A1) daily snow albedo product over the Greenland ice sheet. Remote Sens. Environ. 105, 155–171.

Stroeve, J., Box, J.E., Wang, Z., Schaaf, C., Barrett, A., 2013. Re-evaluation of MODIS MCD43 Greenland albedo accuracy and trends. Remote Sens. Environ. 138, 199–214.

Sturm, M., Douglas, T., Racine, C., Liston, G.E., 2005. Changing snow and shrub conditions affect albedo with global implications. J. Geophys. Res. 110, G01004.

Wang, X., Zender, C.S., 2010. MODIS snow albedo bias at high solar zenith angle relative to theory and to in situ observations in Greenland. Rem. Sens. Environ. 114, 563–575. http://dx.doi.org/10.1016/j.rse.2009.10.014.

Warren, S.G., 1982. Optical properties of snow. Rev. Geophys. Space Phys. 20, 67–89.

Williamson, S.N., Hik, D.S., Gamon, J.A., Kavanaugh, J.L., Koh, S., 2013. Evaluating the quality of clear-sky MODIS Terra daytime Land Surface Temperatures (LST) using ground based meteorology station observations. J. Clim. 26, 1551–1560.

Williamson, S.N., Barrio, I.C., Hik, D.S., Gamon, J.A., 2016. Phenology and species determine growing season albedo increase at the altitudinal limit of shrub growth in the sub-Arctic. Glob. Change Biol. http://dx.doi.org/10.1111/gcb.13297.

Wolfe, R., Nishihama, M., Fleig, A.J., Kuyper, J.A., Roy, D.P., Storey, J.C., Patt, F.S., 2002. Achieving sub-pixel geolocation accuracy in support of MODIS land science. Remote Sens. Environ. 83, 31–49.